Supporting Information

Ishida et al. 10.1073/pnas.1318431110

SI Materials and Methods

Mice. RIP1–Tag2 mice that carry simian virus 40 tumor antigen under a rat insulin promoter have been backcrossed for >60 generations in a C57BL/6J background. All mouse studies were conducted in accordance with protocols approved by the Institutional Animal Care and Use Committee at the University of California, San Francisco and by the veterinary office of the Canton of Vaud, Switzerland.

Tumor Burden, Vascularity, Proliferation, and Apoptosis. Assessment of tumor burden has been described (1). Tumor vascularity was determined as reported (2). BrdU and TUNEL detection assays for proliferation and apoptosis, respectively, were performed as described (3).

Cell Culture. All of the cells were grown at 37 °C with 5% (vol/vol) CO_2, in DMEM supplemented with 10% (vol/vol) FBS and penicillin/streptomycin.

Cell Proliferation. A total of 1×10^5 cells were plated in triplicate in a 12-well plate and incubated for 24 h before addition of a compound. The number of viable cells was determined at the time of drug addition and after 24 h by using Countess Automated Cell Counter (Invitrogen).

Cell-Cycle Analysis. Log-phase cells grown in a six-well plate were treated with 10 μM tetrathiomolybdate (TM) for 24 h. For fixation, cell were trypsinized and collected, washed with cold PBS, and incubated in 1 mL of 70% ethanol in PBS for 30 min at 4 °C. Fixed cells were washed with 5 mL of cold PBS, resuspended in 0.5 mL of cold PBS, and treated with 2 μL of DNase-free RNase (500 mg/mL) for 30 min at 37 °C. To stain DNA, 10 μL of 2 mg/mL propidium iodide was added at room temperature 5–10 min before sorting by a flow cytometer. A total of 35,000 events were recorded. Dean–Jett–Fox model was used to fit the data, from which the fraction of cells in G1, S, and G2 was obtained.

Cytochrome *c* Oxidase Activity, Metabolites, Mitochondrial Membrane Potential, and Lipid Peroxidation. Mitochondria were prepared with the Mitochondria Isolation Kit (Pierce). Cytochrome *c* oxidase activity, ATP, lactate, glucose, and $NADP^+$/NADPH levels were determined with CYTOCOX1 (Sigma), the ATP Somatic Cell Assay Kit (Sigma), the Lactate Assay Kit II (BioVision), the Glucose Assay Kit (Sigma), and the $NADP^+$/NADPH Assay Kit (Bioassay Systems), respectively. Mitochondrial membrane potential was determined by measuring tetramethylrhodamine methyl ester at 150 nM, a fluorescent membrane-permeable cationic probe whose accumulation in the matrix is driven by membrane potential. Cells were treated with 10 μM TM for 24 h before analyses. Lipid peroxidation levels in tumors were determined by measuring the major toxic product of lipid peroxidation, 4-hydroxy-2-nonenal (HNE), using OxiSelect HNE–His Adduct ELISA Kit (Cell Biolabs).

Western Blotting. Cells were lysed on ice with chilled radioimmunoprecipitation assay buffer containing protease inhibitors and phosphatase inhibitors. After sonication, samples were spun at top speed for 10 min at 4 °C. Supernatants were collected, and protein concentrations were measured with the BC Protein Assay kit (BioRad). A total of 20 μg of protein was loaded in each well. Membranes were blocked in 5% (vol/vol) BSA in Tris-buffered saline with Tween-20 (TBST) for 1 h, followed by an overnight incubation with primary antibodies (1:1,000) in 1% (vol/vol) BSA/TBST at 4 °C. Secondary antibodies were used at 1:5,000 in 1% (vol/vol) BSA/TBST. Antibodies against phosphorylated AMPKα (Thr-172), phosphorylated acetyl-CoA carboxylase, and AMPK were from Cell Signaling. Secondary antibodies were from Jackson ImmunoResearch Laboratories.

Cytochrome *c* Oxidase (Complex IV) Activity Staining. Cytochrome *c* oxidase activity staining of tumors was performed as described (4). All tissue sections were subjected to 10 min of reaction with the same batch of COX incubation solution [10 mg of cytochrome C (Sigma-Aldrich), 10 mg of 3,3′-diaminobenzidine tetrahydrochloride hydrate (Sigma-Aldrich), and 2 mg of catalase (Sigma-Aldrich) dissolved in 10 mL of 25 mM sodium phosphate buffer 3,3′-diaminobenzidine tetrahydrochloride hydrate (DAB)]. COX activity in tumors, manifested as brown-colored oxidation product of DAB, was quantified by manually defining tumor areas and measuring the density of the DAB-positive structures with the biological-image analysis program Fiji (5).

Positron Emission Tomography. In vivo measurement of glucose uptake by pancreatic tumors was performed with positron emission tomography (PET). At 15 wk of age, mice were anesthetized with a mixture of 1.5% (vol/vol) isoflurane in 100% O_2 (0.9 L/mL, 2.5 bars), and a catheter was cannulated into the tail vein from which initial values of glycemia were obtained. Fifty-minute list mode acquisitions were acquired with the field of view (FOV) centered on the mouse midsection and initiated with i.v. injection of ^{18}F-fluorodeoxyglucose (^{18}FDG) (~50 MBq) through the tail vein catheter within the first 10 s of the PET scan, followed by 100–500 μL of saline chase solution. Imaging was performed using an avalanche photodiode micro-PET scanner (LabPET4; Gamma Medica). During the entire scanning period, mice were maintained under 1% (vol/vol) isoflurane anesthesia in oxygen delivered at 0.9 L/min using a face mask with constant monitoring of temperature and breathing rate. An energy window of 250–650 keV and a coincidence timing window of 22.2 ns were used. The list mode data were sorted into 1-min time frames of 50 min. The amount of ^{18}FDG activity in the FOV, which is related to the amount of single events per second detected by the scanner, was used to evaluate and control the i.v. delivery of substrate. For image reconstruction, storage of coincidence events recorded in list mode files during the PET scan were binned according to their line of response, i.e., histogramming using an iterative maximum likelihood expectation maximum-based image reconstruction algorithm in a cylindrical volume of 46 mm in diameter and 3.7 cm in length. Voxel size measured $0.5 \times 0.5 \times 1.2$ mm, giving a typical resolution of 1.2 mm at the center of the FOV. After correction for the different count rates of each line of response and quantitative calibration of ^{18}FDG, images of accumulated intracellular ^{18}FDG–6-phosphate at steady state were quantitatively expressed using the standardized uptake value, defined as [mean region of interest (ROI) activity (kBq/cm^3)]/[injected dose (kBq)/body weight (g)]. Images were corrected for nonuniformity of the scanner response, dead time count losses, and physical decay to the time of injection. No correction was applied for attenuation and partial-volume effects. Images were analyzed with PMOD software (Version 3.2; PMOD Technologies). ROIs were drawn manually by optical reading of well-delineated tumors from the dorsal

to ventral plane of the animal centered at midsection at 1-mm intervals.

Quantitative PCR. Total RNA was prepared with the RNeasy Mini (Qiagen) following the manufacturer's recommendations. DNase treatment and RNA cleanup were performed with the DNA-Free RNA Kit (Zymo Research). cDNA synthesis was performed with the iScript cDNA Synthesis Kit (BioRad). Quantitative real-time PCR was performed with the following TaqMan assays (Applied Biosystems): Mm00442036_ m1 (*Twist1*), Mm01171507_m1 (*Sesn3*), Mm01281447_m1 (*Vegfa*), and Mm00452754_m1 (*L19*). Quantitative PCR reactions were performed on Rotor-Gene Q (Qiagen). Ct values were determined and subtracted to obtain the ΔCt [ΔCt = Ct(test locus) – Ct(control locus)]. Relative fold difference was calculated as $2\Delta^{Ct} \times 100$.

1. Inoue M, Hager JH, Ferrara N, Gerber H-P, Hanahan D (2002) VEGF-A has a critical, nonredundant role in angiogenic switching and pancreatic β cell carcinogenesis. *Cancer Cell* 1(2):193–202.
2. Ishida S, McCormick F, Smith-McCune K, Hanahan D (2010) Enhancing tumor-specific uptake of the anticancer drug cisplatin with a copper chelator. *Cancer Cell* 17(6): 574–583.
3. Lopez T, Hanahan D (2002) Elevated levels of IGF-1 receptor convey invasive and metastatic capability in a mouse model of pancreatic islet tumorigenesis. *Cancer Cell* 1(4):339–353.
4. Whitaker-Menezes D, et al. (2011) Hyperactivation of oxidative mitochondrial metabolism in epithelial cancer cells in situ: Visualizing the therapeutic effects of metformin in tumor tissue. *Cell Cycle* 10(23):4047–4064.
5. Schindelin J, et al. (2012) Fiji: An open-source platform for biological-image analysis. *Nat Methods* 9(7):676–682.

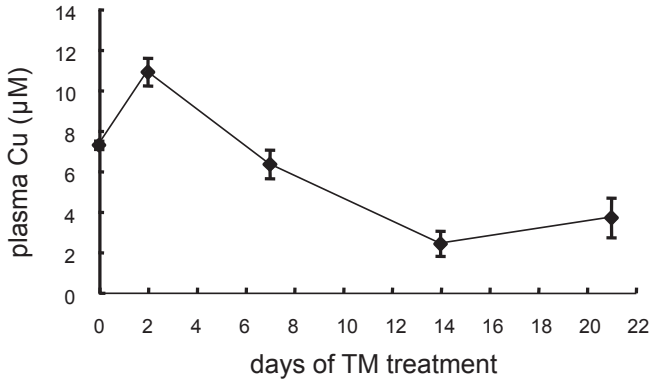

Fig. S1. Plasma copper concentration of RIP1–Tag2 males that were subjected to 1 mg of TM orally once a day for indicated periods ($n = 8$). Copper levels were measured by inductively coupled plasma mass spectrometry (ICP-MS).

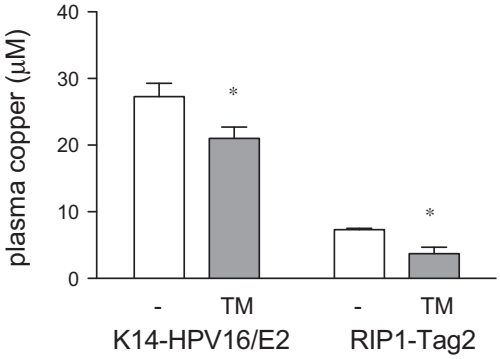

Fig. S2. Effect of the copper chelator TM on plasma copper in different mouse models. Plasma copper was measured by ICP-MS in end-stage K14-HPV16/E_2 females (cervical carcinoma, FVB/n, 6 mo old, $n = 11$) and RIP1–Tag2 males (pancreatic islet carcinoma, C57BL/6, 15 wk old, $n = 8$) following a 3-wk daily treatment with 1 mg of TM. *$P < 0.05$.

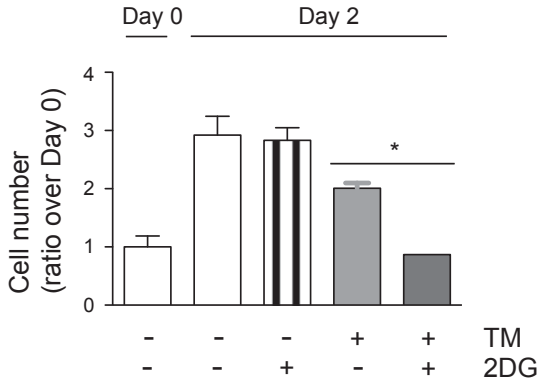

Fig. S3. Effect of TM and the glycolysis inhibitor 2-deoxy-D-glucose (2DG) on proliferation of βTC3 cells. Cells were treated with 10 μM TM and/or 2 μM 2DG for 48 h. Data are means and SEM ($n = 3$). *$P < 0.05$.

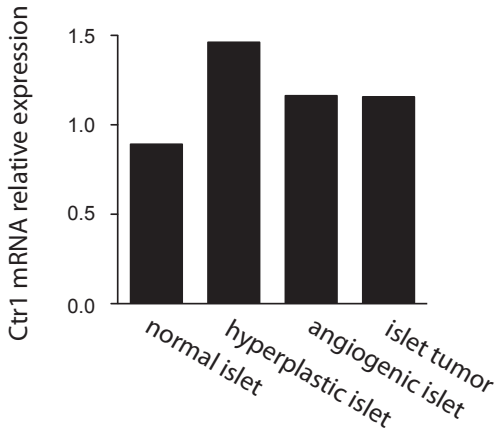

Fig. S4. mRNA levels of the copper transporter Ctr1 in islets of wild-type mice (normal islet) and islets from different stages of tumorigenesis in RIP1–Tag2 mice (hyperplastic islet, angiogenic islet, islet tumor). β-glucuronidase (GUS) gene was used as an endogenous control for TaqMan analysis.